Phonon anomalies and charge dynamics in $Fe_{1-x}Cu_xCr_2S_4$ single crystals

T. Rudolf,[1] K. Pucher,[1] F. Mayr,[1] D. Samusi,[2] V. Tsurkan,[1,2] R. Tidecks,[3] J. Deisenhofer,[1] and A. Loidl[1]
[1]*EP V, Center for Electronic Correlation and Magnetism, University of Augsburg, 86135 Augsburg, Germany*
[2]*Institute of Applied Physics, Academy of Sciences of Moldova, MD 2028, Chisinau, Republic of Moldova*
[3]*Institute of Physics, University of Augsburg, 86135 Augsburg, Germany*
(Received 14 May 2004; revised manuscript received 3 December 2004; published 20 July 2005)

A detailed investigation of phonon excitations and charge carrier dynamics in single crystals of $Fe_{1-x}Cu_xCr_2S_4$ ($x=0,0.2,0.4,0.5$) has been performed by using infrared spectroscopy. In $FeCr_2S_4$ the phonon eigenmodes are strongly affected by the onset of magnetic order. Despite enhanced screening effects, a continuous evolution of the phonon excitations can be observed in the doped compounds with $x=0.2$ (metallic) and $x=0.4,0.5$ (bad metals), but the effect of magnetic ordering on the phonons is strongly reduced compared to $x=0$. The Drude-type charge-carrier contribution to the optical conductivity in the doped samples indicates that the colossal magnetoresistance effect results from the suppression of spin-disorder scattering.

DOI: 10.1103/PhysRevB.72.014450 PACS number(s): 75.47.Gk, 72.15.−v, 72.20.−i, 78.30.−j

I. INTRODUCTION

The discovery of colossal magnetoresistance (CMR) in perovskite-type manganites has attracted considerable attention.[1–5] Double-exchange (DE) mechanism,[6,7] strong electron-phonon coupling,[7] phase separation scenarios[8] or a Griffiths singularity[9] were suggested to clarify the origin of the CMR effect, but a conclusive microscopic model has not yet been established. Ever since, the occurrence of CMR effects has been reported for various other classes of materials, such as pyrochlores,[10] rare-earths based compounds like GdI_2,[11] and ternary chalcogenide spinels ACr_2S_4.[12] These CMR materials have been classified in terms of spin-disorder scattering and a universal dependence of the magnetoresistance vs carrier density has been suggested on theoretical grounds.[13,14]

Ramirez *et al.* drew attention to the spinel system $Fe_{1-x}Cu_xCr_2S_4$ in 1997.[12] In polycrystalline $FeCr_2S_4$ with $T_C=170$ K, the CMR effect reaches values comparable to those observed in perovskite oxides. The substitution of Fe by Cu increases T_C to temperatures above room temperature, and the CMR effect remains relatively strong ($\sim 7\%$).[12] In addition, solid solutions of the ferrimagnetic semiconductor $FeCr_2S_4$ and the metallic ferromagnet $CuCr_2S_4$ show a number of puzzling properties. From the very beginning, a controversial discussion has been arising as to whether the Cu ions are monovalent or divalent for $x \geqslant 0.5$.[15–17] For $x<0.5$ it was established that only monovalent and hence diamagnetic (d^{10}) Cu exists in the mixed crystals.[18] Moreover, $Fe_{1-x}Cu_xCr_2S_4$ shows two metal-to-insulator transitions as a function of x, as the room-temperature resistivity reveals two minima at $x=0.2$ and $x=1$ and concomitantly the Seebeck coefficient changes sign two times.[15,19] Additionally, band-structure calculations predicted that the $Fe_{1-x}Cu_xCr_2S_4$ system should exhibit a half-metallic nature.[17,20,21]

Recent experimental investigations of $Fe_{1-x}Cu_xCr_2S_4$ single crystals indicated a strong dependence of their magnetic and magnetotransport properties on hydrostatic pressure suggesting a strong magnetoelastic coupling.[22,23] Measurements on the ac susceptibility in pure $FeCr_2S_4$ exhibited a cusp in the low-field magnetization, and the onset of magnetic irreversibilities at 60 K was explained by domain-reorientation processes.[24] Later on, ultrasonic studies indicated an anomaly in the temperature dependence of the shear modulus close to 60 K, and it was suggested that the onset of orbital order induces a structural distortion at this temperature.[25] This result, however, is hardly compatible with the observation that orbital order is established in polycrystals close to 10 K, while an orbital glass state is found in single crystals.[26]

Optical spectroscopy simultaneously probes the lattice and electronic degrees of freedom and is, therefore, ideally suited to investigate structural phase transitions and to clarify the importance of electron-phonon coupling for the CMR effect.[27] Earlier infrared (IR) studies in polycrystalline $FeCr_2S_4$ reported, in accordance with the crystal-lattice symmetry $Fd3m$, the existence of four IR-active phonons, which strongly depend on temperature near and below T_C.[28,29] We performed measurements of the optical properties of single crystals of $Fe_{1-x}Cu_xCr_2S_4$ ($x=0$, 0.2, 0.4, and 0.5) to shed light on the interplay of structural and electronic properties in these compounds. Since the optical properties of the samples with $x=0.4$ and $x=0.5$ were found to be very similar, we show and discuss only the corresponding data for $x=0.5$ in the following.

II. EXPERIMENTAL DETAILS

Single crystals of $Fe_{1-x}Cu_xCr_2S_4$ were grown using a chemical transport-reaction method with chlorine as transport agent and the ternary polycrystals as starting material. Details of the sample preparation are described elsewhere.[17] No indication for the existence of secondary phases was found by x-ray diffraction analysis of powdered single crystals. X-ray single-crystal analysis confirmed the high structural homogeneity of the samples. The composition and homogeneity of the samples were examined by electron-probe microanalysis. The samples were optically polished platelets with dimensions of about $3\times5\times1$ mm^3. Structural, magnetic, and electrical transport data are given in Ref. 23.

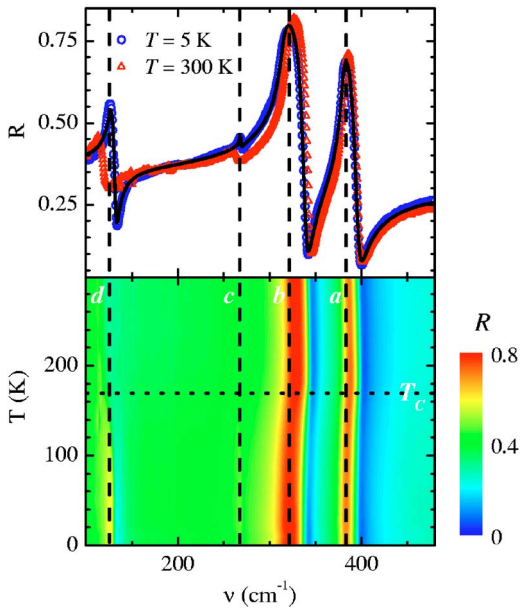

FIG. 1. (Color online) Upper panel, reflectivity R of $FeCr_2S_4$ vs wave number for $T=5$ K and 300 K. A fit of the reflectivity for $T=5$ K is indicated by the solid line. Lower panel, 2D-contour plot of the reflectivity R vs ν and T generated by interpolation of 17 spectra. The vertical lines are highlighting the maxima of the IR-active phonons in R at 5 K.

Two Fourier-transform-infrared spectrometers with a full bandwidth from 10 to 8000 cm^{-1} (BRUKER IFS 113v) and 500 to 42000 cm^{-1} (BRUKER IFS 66v/S) together with a ^{4}He cryostat (OXFORD Optistat) were used for measurements of the optical reflectivity in the energy range from 70 to 30 000 cm^{-1} due to small sample dimensions and for temperatures of $5\ K<T<300$ K. In order to investigate small fractions of the sample surface in the range of 0.1 mm^2 we utilized an IR microscope (BRUKER IRscope II), which works in the far- (FIR) and mid-infrared (MIR) range.

III. EXPERIMENTAL RESULTS AND DISCUSSION

A. Phonon excitations

Figure 1 shows the temperature dependence of the FIR reflectivity R vs wave number of pure $FeCr_2S_4$. In the upper panel R is plotted for 5 and 300 K. The four visible phonon peaks are attributed to the four IR-active F_{1u} modes (symmetry group $Fd3m$, No. 227).[28] To analyze the spectra, we used a four-parameter fit assuming frequency-dependent damping constants to account for the asymmetry of the phonon peaks. This fitting procedure infers a splitting of the longitudinal and transverse eigenfrequencies, ω_L and ω_T, and the corresponding damping constants, Γ_L and Γ_T.[30] The resulting curves describe the measured reflectivity down to 100 cm^{-1} very well, without assuming an additional contribution of free charge carriers. A representative result of these fits is shown by the solid line in the upper panel of Fig. 1 for $T=5$ K. The detailed temperature dependence of the reflectivity is visualized in the two-dimensional (2D) contour plot in the lower panel of Fig. 1. To enable a comparison of the phonon shift, the peak positions (maxima in R) for $T=5$ K are indicated as vertical lines. Around $T_C=167$ K a shift of the phonon frequencies can be observed, especially for the mode d close to 100 cm^{-1}. The intensity of this mode strongly depends on temperature, too (see upper frame of Fig. 1).

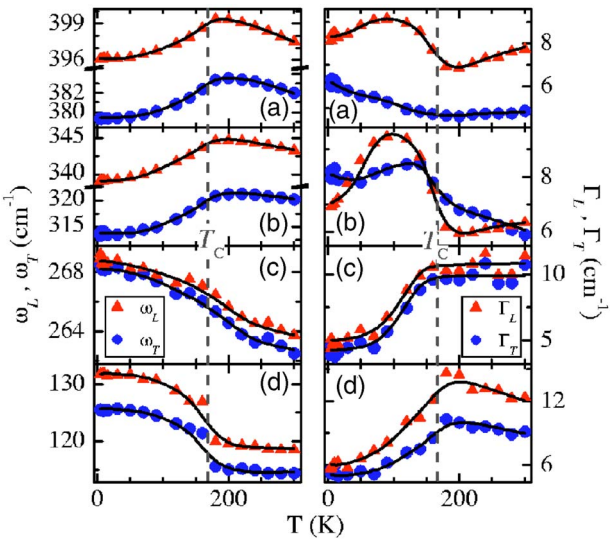

FIG. 2. (Color online) Temperature dependence of the longitudinal (transverse) resonance frequencies ω_L (ω_T) and damping constants Γ_L (Γ_T) obtained by a four-parameter fit for the four IR-active phonons in $FeCr_2S_4$ as described in the text. All solid lines are drawn to guide the eye.

The resonance frequencies ω_L and ω_T (left frames) and the corresponding damping rates Γ_L and Γ_T (right frames) are shown in Fig. 2 as a function of temperature. Above the Curie temperature $T_C=167$ K, the resonance frequencies ω_L and ω_T of all modes reveal a similar quasilinear increase with decreasing temperature, which can be fully ascribed to anharmonic contributions to the lattice potential.[31] In contrast to the rather usual behavior in the paramagnetic regime, modes a and b soften for temperatures below T_C, while ω_L and ω_T increase towards lower temperatures in the case of modes c and d. These anomalous changes of the eigenfrequencies in the vicinity of T_C suggest a correlation with the onset of magnetic order. However, it must be stated that the size of the effect is different for the observed modes; $\Delta\omega=[\omega(T=T_C)-\omega(T=0\ \mathrm{K})]/\omega(T=0\ \mathrm{K})$ is of the order of +3% for the internal mode d, $\lesssim+1\%$ for the bending mode b, approximately -1.5% for the bending mode c, and -1% for the stretching mode a. Longitudinal and transverse eigenfrequencies behave rather similarly.

The influence of magnetic order on phonons in magnetic semiconductors has been proposed by Baltensperger and Helman[32] and Baltensperger[33] more than 30 years ago, and has recently been used by Sushkov *et al.* to describe the phonon spectra in $ZnCr_2O_4$.[34] Based on a model calculation, where superexchange interaction between the magnetic ions infers a spin-phonon coupling, relative frequency shifts up to 10^{-2} have been predicted. The order of magnitude of this effect corresponds nicely to the experimentally observed values in $FeCr_2S_4$ and, therefore, Wakamura[29] considered this

mechanism to dominate the phonons' behavior for $T \lesssim T_C$. Subsequently, Wakamura and co-workers[31,35] discussed the sign of the relative frequency shift in terms of nearest-neighbor FM exchange and next-nearest-neighbor AFM exchange for $CdCr_2S_4$, which exhibits phonon modes with a similar temperature dependence as $FeCr_2S_4$. Moreover, they could show that these anomalous changes in the phonon frequencies are absent in nonmagnetic $CdIn_2S_4$, further corroborating their approach.[35] Thus, the positive shift of modes *a* and *b* would indicate that FM exchange (Cr—S—Cr) dominates in accordance with a strong influence of the (Cr—S) force constants on these modes, and, correspondingly, the negative shift of modes *c* and *d* favors AFM exchange (Cr—S—Cd—S—Cr) with a strong influence of the (Cd—S) force constants. Note that a more rigorous theoretical treatment of anharmonic spin-phonon and phonon-phonon interactions in cubic spinels by Wesselinova and Apostolov[36] confirms the above interpretation. In $FeCr_2S_4$ the interpretation of the effect of magnetic ordering on the IR active phonon modes becomes even more complicated, because there exist, besides FM nearest-neighbor Cr—S—Cr bonds, additional exchange paths via AFM Fe—S—Fe and Fe—S—Cr—S—Fe bonds. Nevertheless, the overall temperature behavior of the phonon frequencies in $FeCr_2S_4$ is similar to $CdCr_2S_4$ and may be well interpreted, accordingly. Note, however, that a critical discussion of the above approach is given by Bruesch and d'Ambrogio.[37]

A straightforward interpretation of the temperature dependence of the damping constants (right panel of Fig. 2) is not obvious at all. Again, considering only the anharmonicity of ionic nonmagnetic crystals, the damping is expected to show some residual low-temperature value and a quasilinear increase in the high-temperature limit, just as observed for the longitudinal damping constants of modes *a* and *b* for $T > T_C$.[29] However, the temperature dependence of Γ_L and Γ_T in general deviates from such a behavior. In the case of mode *d* both damping constants show a broad maximum just above T_C and a steep decrease towards lower temperature for $T < T_C$. Mode *c* follows a similar temperature dependence for $T < T_C$, but the reduction of the damping constants is slightly smaller, and in the paramagnetic regime Γ_L and Γ_T remain almost constant in contrast to the results of Wakamura.[29] The behavior of modes *a* and *b* for $T \lesssim T_C$ appears even more complex, but one can identify the onset of enhancement damping close to $T_C = 170$ K followed by broad cusplike maxima close to 100 K, except for ω_T of mode *a* that increases linearly with decreasing temperatures.

Wakamura[29] argues that the maxima of mode *d* (and *c*) are due to spin fluctuations of the Fe spins, in agreement with the strong influence of the corresponding force constant on this mode according to Bruesch and d'Ambrogio.[37] Furthermore, long range spin order assumingly leads to the anomalous changes of the damping constants for all modes below T_C. In comparison to the temperature dependences of the damping constants in $CdCr_2S_4$, one finds that modes *c* and *d* behave similar to the case of $FeCr_2S_4$.[31] On the other hand, modes *a* and *b* in $FeCr_2S_4$ clearly reveal a more complex behavior than in $CdCr_2S_4$, indicating a significant influence of the iron sublattice and the additional effective exchange coupling between Fe—Fe and Fe—Cr ions on these modes.

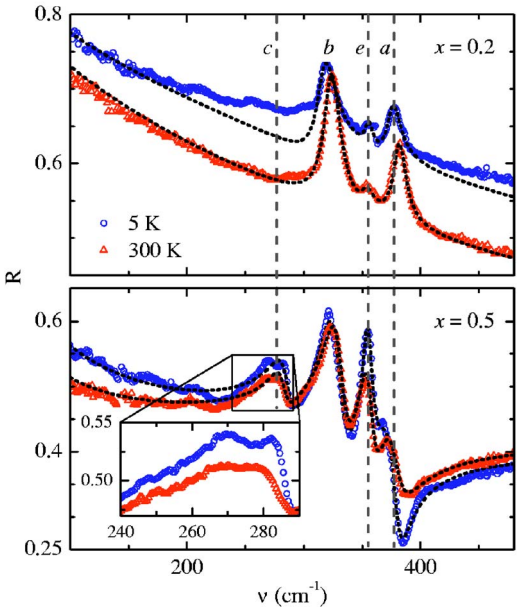

FIG. 3. (Color online) Reflectivity *R* vs wave number for $Fe_{1-x}Cu_xCr_2S_4$ with $x=0.2$ (upper panel) and $x=0.5$ (lower panel) at $T=5$ K (open circles) and $T=300$ K (open triangles). The dashed lines represent results of fits as described in the text.

Additionally, we want to mention the large increase in intensity (about 20%) for mode *d* (close to 120 cm^{-1}) when cooling from room temperature to 5 K (see Fig. 1). The intensity remains almost constant above 200 K, while a linear increase with decreasing temperature is observed below 200 K. At this temperature, maxima appear in the temperature dependence of the damping constants, suggesting a correlation of the two phenomena with regard to the spin-fluctuation scenario discussed above.

When adopting the overall interpretation of the data in terms of spin-phonon coupling, one must consider, however, that, e.g., the appearance of the cusps in the damping constants may be connected to domain reorientation processes visible in the ac susceptibility[24] and anomalies detected by ultrasonic investigations.[25] Although the absence of significant changes of the phonon frequencies contradicts the scenario of a structural phase transition at 60 K driven by orbital ordering as suggested in Ref. 25, it becomes clear that the complex mechanisms dominating the damping effects demand further theoretical studies to single out the important contributions in detail.

Having discussed the phonon properties of pure $FeCr_2S_4$ we now turn to the temperature dependence of the phonon modes for $Fe_{1-x}Cu_xCr_2S_4$. Figure 3 shows the FIR reflectivity for $x=0.2$ (upper panel) and $x=0.5$ (lower panel) for temperatures 5 K and 300 K each. The results for $x=0.4$ are very similar to those obtained for $x=0.5$ and, hence, only the data for $x=0.5$ is shown and discussed. The reflectivity of both samples, $x=0.2$ and 0.5, shows a Drude-type contribution due to the presence of free charge carriers, while $FeCr_2S_4$ can be described as an insulator. The highest Drude-type conductivity is found for $x=0.2$ and the phonon modes are on the verge of being fully screened. For both compounds the internal mode *d* at ~ 120 cm^{-1} (see Fig. 1 for the

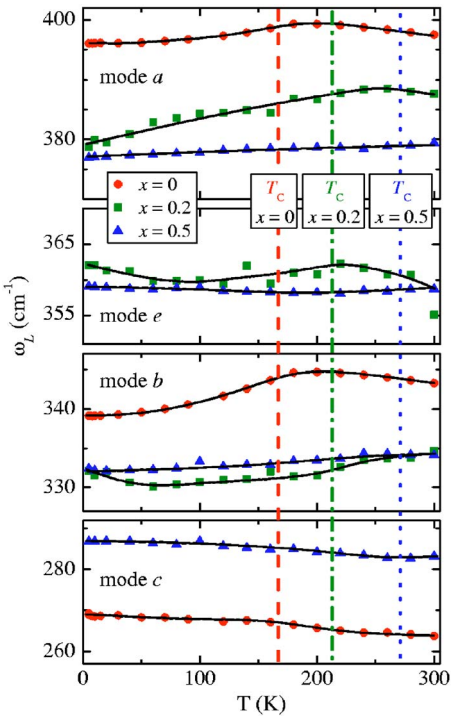

FIG. 4. (Color online) Temperature dependence of the longitudinal eigenfrequencies ω_L of the IR-active phonon modes in $Fe_{1-x}Cu_xCr_2S_4$ for $x=0$ (circles), 0.2 (squares), and 0.5 (triangles). The dashed ($x=0$), dashed-dotted ($x=0.2$), and dotted lines ($x=0.5$) indicate the magnetic transition temperatures. The solid lines are drawn to guide the eye.

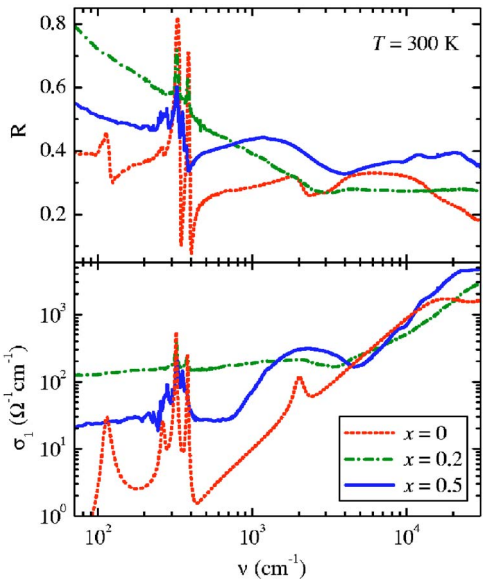

FIG. 5. (Color online) Upper panel, semilogarithmic plot of the room-temperature reflectivity vs wave number in $Fe_{1-x}Cu_xCr_2S_4$ for Cu concentrations $x=0$, 0.2, and 0.5. Lower panel, double-logarithmic plot of the real part of the dynamic conductivity σ_1 as derived from the reflectivity spectra.

pure compound) can hardly be detected. Focusing on the group of external modes, a new mode *e* appears close to 350 cm^{-1}, while on increasing Cu concentration x mode *a* at 380 cm^{-1} becomes considerably reduced in intensity. Without an accompanying lattice dynamical calculation one cannot decide if this new mode represents an impurity mode due to the doping with Cu or a symmetry change. There are reports in literature[15,38] claiming the reduction of symmetry to $F\bar{4}3m$ because of the ordering of Fe and Cu ions on the *A* sublattice. In this case seven IR-active phonon modes are predicted. Assuming that the peak close to 275 cm^{-1} (mode *c*) is generated by two single phonon modes (see inset in Fig. 3), only five modes are visible, while the internal mode *d* close to 120 cm^{-1} remains screened. However, our results rather point toward a continuous evolution of the phonon modes on increasing x and favor a statistical *A*-site distribution of Cu and Fe ions throughout the lattice instead of a symmetry reduction resulting from a superstructure due to an ordered *A* sublattice.

We tried to fit the complete spectra taking into account the reflectivity up to 10 000 cm^{-1}, using a four-parameter fit for the phonon modes and a Lorentz oscillator for the mid-infrared excitation at about 2500 cm^{-1} (see the next section). Representative results of these fits at low wave numbers are shown in Fig. 3 as dashed lines. The temperature dependences of the longitudinal modes ω_L as derived from these fits are shown in Fig. 4 together with corresponding data for $x=0$. The transverse eigenfrequencies behave rather similarly (not shown). Compared to the sample with $x=0$, the temperature dependence of the damping constants in the doped compounds is weak and therefore not shown here either. Regarding the sample with $x=0.2$ similar anomalies as in pure $FeCr_2S_4$ can be seen in the vicinity of T_C for the observable modes *a*, *b*, and *e*. Obviously, the temperature dependence of all phonon frequencies for $x=0.5$ is very weak and no clear anomalies around T_C are visible. Within the experimental uncertainties one can detect a slight decrease of ω_L towards lower temperatures except for mode *c*, which behaves similarly to the case of $FeCr_2S_4$ (compare Fig. 2).

Keeping in mind the influence of spin fluctuations and spin-phonon coupling on the phonon properties in $FeCr_2S_4$, Cu doping seems to reduce these features significantly. This observation is in agreement with reduced spin-orbit coupling due to the substitution of Jahn-Teller active Fe^{2+} by non-Jahn-Teller active Fe^{3+}. Therefore, for $x=0.5$ only Fe^{3+} with a half-filled *d*-shell is present in the system[17,39] and the system becomes almost magnetically isotropic as it was confirmed by ferromagnetic resonance experiments.[23]

B. Dynamic conductivity and electronic excitations

When the reflectivities of the doped compounds with Cu concentrations $x=0.2$ and 0.5 (Fig. 3) are compared with that of pure $FeCr_2S_4$ it becomes clear that contributions from free charge carriers must be taken into consideration. The metallic-like behavior is most significant for $x=0.2$, but it becomes reduced again on further doping. For a consistent description of the Drude-type behavior of the doped compounds, it is important to measure the reflectivity spectra to higher energies. The room-temperature reflectivities of $Fe_{1-x}Cu_xCr_2S_4$ for $x=0.2$ and 0.5 are plotted in the upper panel of Fig. 5 up to 3×10^4 cm^{-1}, corresponding to almost 4 eV, and are com-

pared to the reflectivity of insulating $FeCr_2S_4$. For the Kramers-Kronig analysis of the smoothed reflectivity data we used a low-frequency Hagen-Rubens extrapolation and a high-frequency extrapolation with a $\nu^{-0.5}$ power law up to 10^6 cm^{-1} and a subsequent ν^{-4} high-frequency tail. The resulting dynamic conductivities $\sigma(\nu)$ are shown in the lower panel of Fig. 5. We carefully checked the high-frequency extrapolation, also trying smoother extrapolations, but found that the results are not influenced in the relevant energy range below 20 000 cm^{-1}. The use of a Hagen-Rubens extrapolation is justified by the fact that we have the complete information on the absolute values of the dc conductivities and the corresponding temperature dependences for all compounds, although we are aware of the additional uncertainties originating from the Hagens-Rubens extrapolation, specifically for the sample with $x=0.5$. However, the best fits of the reflectivity at room temperature, even in the limited spectral range, yielded dc conductivities of 150 $(\Omega\,\mathrm{cm})^{-1}$ for $x=0.2$ and 35 $(\Omega\,\mathrm{cm})^{-1}$ for $x=0.5$, close to the dc values derived from the four-probe measurements on single crystals by Fritsch *et al.*[23]

For $x=0$ a weak but well-defined electronic transition is observed close to 2000 cm^{-1} and a further transition appears close to 20 000 cm^{-1} ($\approx$2.5 eV). On substituting iron by copper, metallic behavior shows up and for $Fe_{0.8}Cu_{0.2}Cr_2S_4$ the dc conductivity is of the order 150 $(\Omega\,\mathrm{cm})^{-1}$. The transition at 2000 cm^{-1} becomes almost fully suppressed for $x=0.2$. Obviously, the *d* electrons become strongly delocalized. It is generally accepted that in an ionic picture monovalent Cu is substituted, inducing trivalent Fe. Our results suggest that the system behaves as if holes are doped into an insulator driving the compound into a metallic regime. Unexpectedly, a broad peak appears again close to 2500 cm^{-1} for $x=0.5$.

The observed doping dependence of the conductivity spectra as documented in Fig. 5 can be compared with band-structure calculations of these compounds.[17,21,39] Local spin-density approximation (LSDA) band-structure calculations predict a half-metallic ground state of $FeCr_2S_4$, with a partly filled *e* band at the Fermi level. Correlation effects via LSDA+*U* yield a splitting of the Fe *e* band into a lower and upper Hubbard band characterizing $FeCr_2S_4$ as a Mott-Hubbard insulator.[21] The splitting of the *e* band is of the order of about 0.5 eV, and, hence, the peak close to 2000 cm^{-1} may be interpreted as a transition between the lower and upper Hubbard band. Accordingly, the high-energy excitation can be attributed to a Cr($3d$) to Fe($3d$) transition.

Using an ionic picture with localized Fe *d* states, alternatively, the transition at 2000 cm^{-1} may correspond to a transition between the lower *e* doublet and the t_2 triplet of the Fe *d* states split in a tetrahedral crystal field. The expected crystal-field splitting for Fe^{2+} located in the tetrahedral site of the spinel structure is rather weak[40] and a splitting of the order 2000–3000 cm^{-1} seems reasonable. Further support for this interpretation comes from the observation of crystal-field transitions as measured for diluted Fe^{2+} in $CdIn_2S_4$. Here a crystal-field splitting of approximately 2500 cm^{-1} has been reported by Wittekoek *et al.*[41]

The appearance of the broad excitation for $x=0.5$ in the mid-infrared region at about 2500 cm^{-1}, however, cannot be explained easily. In an ionic picture only trivalent iron and monovalent copper are expected for $x=0.5$,[15,16] and recent x-ray photoelectron spectroscopy[18] strongly favors the existence of only monovalent Cu for $x=0.5$. Therefore, one can exclude the possibility that the broad excitation may be attributed to Fe^{2+} similarly to the well-defined electronic excitation for $x=0$. Nevertheless, it has been concluded from Mössbauer experiments in $Fe_{1-x}Cu_xCr_2S_4$ that an ionic picture is not applicable at all.[42] For $x=0.3$ and $T<T_C$ the complicated Mössbauer spectra indicate two different Fe sites corresponding to Fe^{2+} and Fe^{3+}, while for $T>T_C$ a single line pointed towards a fast electron exchange between these two sites. For $x=0.5$ the line pattern for $T>T_C$ evidenced the existence of Fe^{3+} and a strong delocalization of the Cu *d*-derived electrons. Hence, further studies beyond the scope of this paper are needed to clarify the nature of this mid-infrared excitation.

In the following we will discuss the optical conductivity results in the low frequency range in comparison with the dc conductivity data reported in Ref. 23. The room-temperature spectra for the concentrations $x=0.2$ and 0.5, shown in Fig. 5 have been used to estimate the Drude-type conductivity. For all temperatures, the spectra could satisfactorily be described using a plasma frequency $\omega_p=12\,000$ cm^{-1} and a dielectric constant $\epsilon_\infty=10.6$ for $x=0.2$, which is close to the value $\epsilon_\infty=11.5$ for $x=0$. For $x=0.5$ we used $\omega_p=5000$ cm^{-1} and an enhanced dielectric constant $\epsilon_\infty=15.5$. The enhanced ϵ_∞ indicates strong changes in the electronic excitation spectrum at higher frequencies, but due to the complexity of the spectrum in this energy region there is also a larger uncertainty in ϵ_∞ for $x=0.5$. The decrease of the plasma frequency by a factor of 2.4 can be explained by a decrease of the charge carrier density, as $Fe_{1-x}Cu_xCr_2S_4$ approaches a metal-to-insulator transition close to $x=0.5$. With these values, the conductivity below 500 cm^{-1} could reasonably be fitted for all temperatures as indicated by the dashed lines in Fig. 3 for the spectra at 5 K and 300 K.

The resulting temperature dependences of the dc conductivity (upper panel) and relaxation rates $\gamma\propto\tau^{-1}$ (lower panel) are shown in Fig. 6. The dc conductivities as derived from four-probe measurements[23] are indicated by solid lines. The dc conductivities were scaled at room temperature, utilizing a factor of 1.6 for $x=0.2$ and a factor of 1.05 for $x=0.5$. Above 100 K the four-probe dc results and the dc values as derived from the optical measurements follow a similar temperature dependence. However, at low temperatures the dc measurements are dominated by localization effects, which appear much weaker in the high-frequency ($>$100 cm^{-1}) derived optical data. That localization effects are most significant in the low-frequency ("dc") transport measurements becomes clear from the fact that in doped semiconductors the conductivity below the FIR regime increases almost linearly with frequency.[43] In the sample with $x=0.5$, which exhibits the lower conductivity, localization effects already dominate at higher temperatures. This may be attributed to a significant decrease of the charge-carrier density and concomitant increase of disorder due to the statistical distribution of the Cu ions in the lattice,[39] further discarding the possibility of

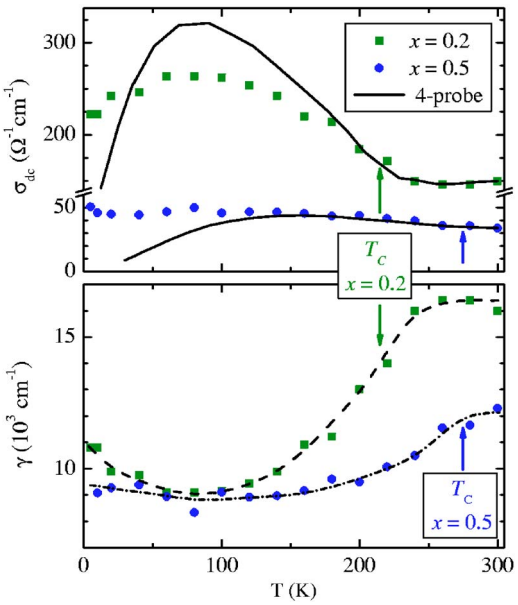

FIG. 6. (Color online) Upper panel, temperature dependence of the dc conductivity of $Fe_{1-x}Cu_xCr_2S_4$ as determined from fits to the reflectivity (see text). The dc conductivities as observed from four-probe measurements (Ref. 23) are indicated by solid lines and were scaled to the room temperature optical values. Lower panel, temperature dependence of the Drude-type relaxation rates. Ferrimagnetic ordering temperatures are indicated by arrows. The dashed and dashed-dotted lines are drawn to guide the eye.

A-site order of Fe and Cu for $Fe_{1-x}Cu_xCr_2S_4$.

Finally, we want to draw attention to the temperature dependence of the relaxation rate γ (lower panel of Fig. 6). In the magnetically ordered state below T_C, the relaxation rates become significantly reduced, e.g., the reduction amounts to almost 50% for $x=0.2$. We recall that the plasma frequency has been kept constant for each compound as a function of temperature. This indicates that the increase of the conductivity just below the magnetic ordering temperature results from the freezing out of disorder scattering and not from a change of the carrier density via band-structure changes at the onset of ferrimagnetic order. Taking into account the classification of chalcogenide spinels ACr_2S_4 as systems where CMR originates from spin-disorder scattering,[13] the observed reduction of the relaxation rate below T_C must be regarded as direct evidence of such a scenario. In external fields the onset of ferrimagnetic order shifts to higher temperatures. Concomitantly, a reduction of the scattering rate and the anomalous increase of the conductivity arise. As a consequence, maximal CMR effects will show up just below T_C as a function of an external magnetic field. A similar scenario has been reported for GdI_4, where the magnetic and magnetotransport properties have been described successfully in terms of spin fluctuations and their suppression by external magnetic fields in the vicinity of T_C.[44,45] We would like to point out that at low temperatures the relaxation rates for $x=0.2$ and $x=0.5$ are of the same order of magnitude $\sim 10^4$ cm^{-1}, indicating a similar level of disorder for the Cu doped compounds.

IV. SUMMARY

In summary, we investigated the optical properties of $Fe_{1-x}Cu_xCr_2S_4$ single crystals for Cu concentrations $x=0$, 0.2, 0.4, and 0.5. Phonon excitations and dynamic conductivity for $x=0.4$ are very similar to the results for $Fe_{0.5}Cu_{0.5}Cr_2S_4$ and were not discussed separately. The phonon excitations were measured as a function of temperature between 5 K and room temperature. Pure $FeCr_2S_4$ shows clear anomalies in the eigenfrequencies at the transition from the paramagnetic to the ferromagnetic state, which can be explained by spin-phonon coupling. Concerning the complex behavior of the damping constants, spin fluctuations in the vicinity of T_C may describe many of the anomalous changes, but further theoretical studies are necessary to corroborate this interpretation. The influence of magnetic order on the eigenmodes is reduced with increasing x, and the appearance of a new phonon mode close to 350 cm^{-1} is attributed to an impurity mode rather than to a symmetry reduction due to *A*-site order.

Moreover, the charge dynamics of $Fe_{1-x}Cu_xCr_2S_4$ were investigated. $FeCr_2S_4$ is an insulator, but becomes metallic when slightly doped with Cu. The conductivity of the free charge carriers can be described by a normal Drude-type behavior. The dc conductivity for $x=0.2$ is enhanced by a factor of 4 in comparison to $x=0.5$. The temperature dependence of the optically derived dc conductivity for both doped compounds is is in good agreement with resistivity measurements, but localization effects at lowest temperatures appear weaker in the optical measurements. The corresponding behavior of the scattering rate, which shows a strong decrease below the ferrimagnetic phase transition, evidences the freezing out of disorder scattering below T_C. In accordance with the proposed classification of the ternary chalcogenide spinels as spin-disorder magnetoresistive materials, the reduction of the relaxation rate corroborates such a scenario and makes clear that spin disorder must be considered a necessary ingredient towards a theoretical description of this fascinating class of materials.

ACKNOWLEDGMENTS

It is a pleasure to thank H.-A. Krug von Nidda, J. Hemberger, and Ch. Hartinger for fruitful discussions. This work was partly supported by the DFG via the Sonderforschungsbereich 484 (Augsburg), by the BMBF/VDI via the Contract No. EKM/13N6917/0, by the U.S. Civilian Research and Development Foundation (CRDF), and by the Moldavian Research and Development Association (MRDA) via Grant No. MP2-3047.

[1] R. M. Kusters, J. Singleton, D. A. Keen, R. McGreevy, and W. Hayes, Physica B **155**, 362 (1989).
[2] Z. Jirák, S. Krupička, Z. Šimša, M. Dlouhá, and S. Vratislav, J. Magn. Magn. Mater. **53**, 153 (1985).
[3] R. von Helmolt, J. Wecker, B. Holzapfel, L. Schultz, and K. Samwer, Phys. Rev. Lett. **71**, 2331 (1993).
[4] K. Chahara, T. Ohno, M. Kasai, and Y. Kozono, Appl. Phys. Lett. **63**, 1990 (1993).
[5] S. Jin, T. H. Tiefel, M. McCormack, R. A. Fastnacht, R. Ramesh, and L. H. Chen, Science **264**, 413 (1994).
[6] C. Zener, Phys. Rev. **82**, 403 (1951).
[7] A. J. Millis, P. B. Littlewood, and B. I. Shraiman, Phys. Rev. Lett. **74**, 5144 (1995).
[8] M. Mayr, A. Moreo, J. A. Vergés, J. Arispe, A. Feiguin, and E. Dagotto, Phys. Rev. Lett. **86**, 135 (2001).
[9] M. B. Salamon, P. Lin, and S. H. Chun, Phys. Rev. Lett. **88**, 197203 (2002).
[10] Y. Shimakawa, Y. Kubo, and T. Manako, Nature (London) **379**, 53 (1996).
[11] C. Felser, K. Ahn, R. K. Kremer, R. Seshadri, and A. Simon, J. Solid State Chem. **147**, 19 (1999).
[12] A. P. Ramirez, R. J. Cava, and J. Krajewski, Nature (London) **386**, 156 (1997).
[13] P. Majumdar and P. Littlewood, Nature (London) **395**, 479 (1998).
[14] G. Gomez-Santos, S. Fratini, and F. Guinea, Phys. Rev. B **70**, 184420 (2004).
[15] F. K. Lotgering, R. P. Van Stapele, G. H. A. M. Van Der Steen, and J. S. Van Wieringen, J. Phys. Chem. Solids **30**, 799 (1969).
[16] J. B. Goodenough, J. Phys. Chem. Solids **30**, 261 (1969).
[17] E. Z. Kurmaev, A. V. Postnikov, H. M. Palmer, C. Greaves, St. Bartkowski, V. Tsurkan, M. Demeter, D. Hartmann, M. Neumann, D. A. Zatsepin, V. R. Galakhov, S. N. Shamin, and V. Trofimova, J. Phys.: Condens. Matter **12**, 5411 (2000).
[18] V. Tsurkan, M. Demeter, B. Schneider, D. Hartmann, and M. Neumann, Solid State Commun. **114**, 149 (2000).
[19] G. Haacke and L. C. Beegle, J. Appl. Phys. **39**, 656 (1968).
[20] W. E. Pickett and J. S. Moodera, Phys. Today **54**, 39 (2001).
[21] M. S. Park, S. K. Kwon, S. J. Youn, and B. I. Min, Phys. Rev. B **59**, 10018 (1999).
[22] V. Tsurkan, I. Fita, M. Baran, R. Puzniak, D. Samusi, R. Szymczak, H. Szymczak, S. Klimm, M. Klemm, S. Horn, and R. Tidecks, J. Appl. Phys. **90**, 875 (2001).
[23] V. Fritsch, J. Deisenhofer, R. Fichtl, J. Hemberger, H.-A. Krug von Nidda, M. Mücksch, M. Nicklas, D. Samusi, J. D. Thompson, R. Tidecks, V. Tsurkan, and A. Loidl, Phys. Rev. B **67**, 144419 (2003).
[24] V. Tsurkan, J. Hemberger, M. Klemm, S. Klimm, A. Loidl, S. Horn, and R. Tidecks, J. Appl. Phys. **90**, 4639 (2001).
[25] D. Maurer, V. Tsurkan, S. Horn, and R. Tidecks, J. Appl. Phys. **93**, 9173 (2003).
[26] R. Fichtl, V. Tsurkan, P. Lunkenheimer, J. Hemberger, V. Fritsch, H.-A. Krug von Nidda, E.-W. Scheidt, and A. Loidl, Phys. Rev. Lett. **94**, 027601 (2005).
[27] Ch. Hartinger, F. Mayr, J. Deisenhofer, A. Loidl, and T. Kopp, Phys. Rev. B **69**, 100403(R) (2004).
[28] H. D. Lutz, G. Waschenbach, G. Kliche, and H. Haeuseler, J. Solid State Chem. **48**, 196 (1983).
[29] K. Wakamura, Solid State Commun. **71**, 1033 (1989).
[30] D. W. Berreman and F. C. Unterwald, Phys. Rev. **174**, 791 (1968).
[31] K. Wakamura and T. Arai, J. Appl. Phys. **63**, 5824 (1988).
[32] W. Baltensperger and J. S. Helman, Helv. Phys. Acta **41**, 668 (1968).
[33] W. Baltensperger, J. Appl. Phys. **41**, 1052 (1970).
[34] A. B. Sushkov, O. Tchernyshyov, W. Ratcliff II, S. W. Cheong, and H. D. Drew, Phys. Rev. Lett. **94**, 137202 (2005).
[35] K. Wakamura, T. Arai, and K. Kudo, J. Phys. Soc. Jpn. **41**, 130 (1976).
[36] J. M. Wesselinowa and A. T. Apostolov, J. Phys.: Condens. Matter **8**, 473 (1996).
[37] P. Bruesch and F. d'Ambrogio, Phys. Status Solidi B **50**, 513 (1972).
[38] H. M. Palmer and C. Greaves, J. Mater. Chem. **9**, 637 (1999).
[39] O. Lang, C. Felser, R. Seshadri, F. Renz, J.-M. Kiat, J. Ensling, P. Gütlich, and W. Tremel, Adv. Mater. (Weinheim, Ger.) **12**, 65 (2000).
[40] A. Abragam and B. Bleaney, *Electron Paramagnetic Resonance of Transition Ions* (Clarendon, Oxford, 1970).
[41] S. Wittekoek, R. P. van Stapele, and A. W. J. Wijma, Phys. Rev. B **7**, 1667 (1973).
[42] G. Haacke and A. J. Nozik, Solid State Commun. **6**, 363 (1968).
[43] P. Lunkenheimer and A. Loidl, Phys. Rev. Lett. **91**, 207601 (2003).
[44] I. Eremin, P. Thalmeier, P. Fulde, R. K. Kremer, K. Ahn, and A. Simon, Phys. Rev. B **64**, 064425 (2001).
[45] J. Deisenhofer, H.-A. Krug von Nidda, A. Loidl, K. Ahn, R. K. Kremer, and A. Simon, Phys. Rev. B **69**, 104407 (2004).